Phase-Shifting Acceleration of Ions in an Ion Cyclotron Resonance Spectrometer: Kinetic Energy Distribution and Reaction Dynamics

Stephen L. Craig and John I. Brauman*

Department of Chemistry, Stanford University, Stanford, California 94305-5080

Received: February 18, 1997; In Final Form: April 14, 1997[⊗]

The kinetic energy distribution of trapped ions in an ion cyclotron resonance spectrometer (ICR) under a periodically phase-reversed rf potential is determined. At the operating pressures typical for the ICR (10^{-7}−10^{-5} Torr), the ions eventually achieve a kinetic energy distribution that varies across short time intervals (0.1 ms) but is constant on the time scale of bimolecular collisions. This provides the opportunity to study quantitatively the translational energy dependence of bimolecular reactions and sequential collisional activation processes. The kinetic energy distribution, although not Maxwell−Boltzmann, is readily calculable. Results obtained for the kinetic energy dependence of the reaction of $Cl^- + CH_3Br$ are qualitatively and quantitatively consistent with reported nonstatistical behavior in that system. Experimental considerations are discussed.

Introduction

It has been known for many years that a resonant radio frequency can be used to accelerate trapped ions in an ion cyclotron resonance (ICR) spectrometer.[1] It is only recently, however, that the acceleration resulting from the application of an rf signal has been quantified theoretically and experimentally.[2−6] As a result, the strength and duration of an rf driving signal may be chosen so that the resonant ions are accelerated to a specified velocity in a "single-shot" experiment. Single-shot acceleration has been used in FT-ICR to measure the threshold energies for collision-induced dissociation and endothermic reactions.[7−12]

The use of the single-shot technique to quantify the translational energy dependence of bimolecular reactions is difficult, however, because the motion of the accelerated ions is cooled by bimolecular collisions. Because this process occurs on the time scale of collisions, it is competitive with, and often much faster than, the bimolecular reaction in which one is interested. The reactant ion population, therefore, is comprised of a mixture of translationally hot and cold ions, and the relative concentration of ions of different energies changes with time. Furthermore, the reactions of the fast and slow ions are observed simultaneously so that deconvoluting the translational energy dependence from such an experiment represents a formidable challenge.

In lieu of a single-shot experiment, it would be advantageous to create a steady-state distribution of accelerated ions so that the kinetics of the reaction could be followed normally by monitoring the decay of the reactant and appearance of product signals. In this paper, we demonstrate that a phase-shifting rf potential can be used to create a distribution of ion kinetic energies that is constant for time scales greater than ∼0.1 ms. Calculation of the kinetic energy (KE) distribution is straightforward, enabling the accurate measurement of the translational energy dependence of bimolecular reactions and collisional activation processes in FT-ICR spectrometry. We use this technique to study the S_N2 reaction of chloride ion with methyl bromide, and the results obtained are in excellent agreement with results of previous examinations of the translational energy dependence of that reaction.

[⊗] Abstract published in *Advance ACS Abstracts,* May 15, 1997.

Background and Theory

The use of a phase-shifting radio frequency to manipulate ion kinetic energies in an ICR has been described previously.[13,14] It is based on the demonstration by Marshall and co-workers[15] that ions accelerated by a resonant radio frequency can be decelerated by a 180° phase shift in the rf signal, a principle that has been applied successfully in "notched" ion ejection,[16−18] ion-skimming techniques,[19] and two-dimensional FT-ICR.[20,21] By repeatedly accelerating and then decelerating ions in alternating succession over long periods of time, the ions remain, on average, excited above thermal translational energies.

The two-dimensional equations of motion for individual ions under rf acceleration conditions have been derived previously. We follow the notation of Hearn, Watson, Baykut, and Eyler[22] in which the *z*-axis is defined by the magnetic field in the ICR cell. We initially consider the motion of ions constrained to the plane $z = 0$ and denote the ion position at time t by $x(t)$ and $y(t)$, where the *y*-axis is defined to be normal to the excitation plates that carry the accelerating signal. All ions are assumed to orbit the center of the cell, $x = y = z = 0$. The "phase" ϕ_1 of a given ion is defined by its position and direction at $t = 0$ by $\cos(\phi_1) = x(0)/(x^2(0) + y^2(0))^{1/2}$. The phase ϕ_2 of the accelerating signal reflects the corresponding "direction" of the rf signal at $t = 0$ so that $\phi_2 = 0$ corresponds to a maximum amplitude along the *y*-axis at $t = 0$.

Given an rf potential of field strength E and assuming that interaction of the rf with the ion is described by the infinite electrode approximation, the position at time t of an ion having initial velocity $v(0)$ in the plane of cyclotron motion and cyclotron frequency ω_c is

$$x(t) = x(0) + \frac{v(0)}{\omega_c}(\sin(\omega_c t - \phi_1) + \sin(\phi_1)) + \frac{qE}{2m\omega_c^2}(\sin(\omega_c t)\cos(\phi_2) - \omega_c t(\cos(\omega_c t + \phi_2)))$$

$$y(t) = y(0) + \frac{v(0)}{\omega_c}(\cos(\omega_c t - \phi_1) - \cos(\phi_1)) - \frac{qE\cos(\phi_2)}{m\omega_c^2} + \frac{qE}{2m\omega_c^2}(\cos(\omega_c t)\cos(\phi_2) + \cos(\omega_c t + \phi_2) + \omega_c t(\sin(\omega_c t + \phi_2))) \quad (1)$$

S1089-5639(97)00602-6 CCC: $14.00

The cyclotron radius $r(t)$ and velocity $v(t)$ of an ion is related to its position $(x(t), y(t))$ by

$$r(t) = (x(t)^2 + y(t)^2)^{1/2}$$

$$v(t) = 2\pi\omega_c r(t)$$

Grosshans and Marshall have demonstrated experimentally that the final cyclotron radius after rf excitation is only 72% of that predicted by the infinite electrode approximation. Because the final kinetic energy is proportional to the square of the radius, the actual kinetic energy is only half that from the calculation using the approximation.[4−6] To accurately determine the trajectories of ions in an rf field, eq 1 must be modified to correct for the error in the infinite electrode approximation. Because the final radius depends nearly linearly on field strength, this is easily accomplished by replacing the actual differential field strength across the excitation electrodes, E, with an effective field strength $E_{\text{eff}} = 0.72E$. All calculations reported in this work use the corrected field strength.

The effect of the rf potential is to drive a resonant ion to larger radii essentially linearly for the duration of the signal (Figure 1a). In our experiments, the duration of this initial driving period is set to N periods of ion cyclotron motion. At the end of N cycles, the phase of the driving signal is reversed by 180° (Figure 1b) so that the ion is now 180° out of phase with the rf signal. The ion is subsequently driven to a progressively smaller radius for another N cycles until it reaches its initial position and the phase of the rf is reversed again.

In the absence of collisions, this process would continue indefinitely and each ion would oscillate between two limiting radii. At nonzero pressure, however, collisions disrupt this process as shown in Figure 2. The effect of the collisions are twofold. First, a collision will change both the energy and direction of the ion translational motion. Because the ions are, on average, translationally excited, collision with a thermal neutral molecule will generally lower the ion kinetic energy and bring it closer to the thermal value.

More importantly, however, the collision displaces the minimum radius of the ion trajectory with respect to the time of the phase reversal. In the absence of collisions, the minimum radius occurs nearly in coincidence with the phase shift, and the rf serves as an accelerating signal for the entire duration of one driving period and then as a decelerating signal for the duration of the next, and so on. A collision in the middle of the excitation sequence, however, will lower the ion cyclotron radius as described above and also take the ion out of phase with the rf. After rephasing, the ion is accelerated by the rf but only for the remainder of the driving period. The ion trajectory now proceeds to a maximum radius that is smaller than for a trajectory in the absence of collisions. After the phase shift, the ion is driven to progressively smaller radii but now reaches $r = 0$ before the next phase shift. The ion is driven through $r = 0$ and then to larger radii *during this same driving period*. The trajectory reaches a second maximum and the phase is shifted again, driving the trajectory back through $r = 0$ and to the previous local maximum. The effect of a collision is depicted in Figure 2. For visual clarity, Figure 2 shows a trajectory in which the ion velocity is reduced to zero in the bimolecular collision. The effect of a collision on the range of radii (and, hence, kinetic energies) accessed by an ion is also shown schematically in Figure 3.

Eventually, nearly all the ions will have undergone at least one collision and their radial trajectories will resemble those shown in Figure 2. The limiting radii of ion motion depend on

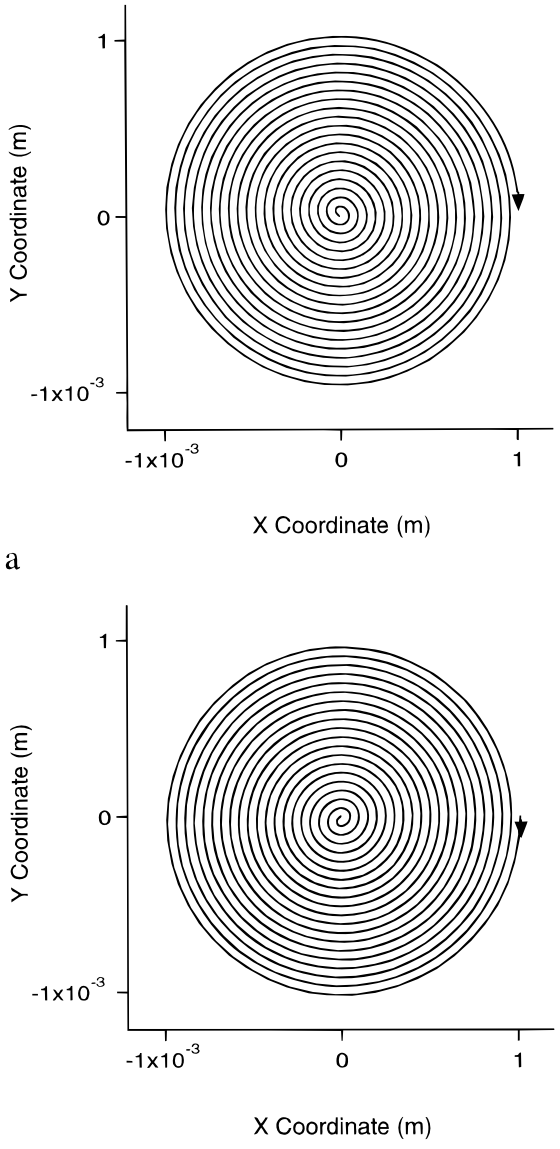

Figure 1. Typical ion trajectory in response to an applied resonant radio frequency. The ion is initially at $x = y = 0$ and is accelerated to progressively larger radii for 20 periods of cyclotron motion (a), at which point the phase of the rf is reversed by 180°. The ion is then driven to progressively smaller radii until it reaches its initial position (b), and the phase is reversed again. In the absence of collisions, this process repeats itself indefinitely. For simplicity, the trajectory shown is calculated for an ion initially at rest, which is not representative. The magnetic field strength is 0.6 T and the rf amplitude is 16 V m^{-1}. Ion cyclotron motion is clockwise, as indicated by the arrows.

at what point in the period of the driving signal the collision occurs, and the phase and radius of the ion cyclotron motion after the collision event. When the phase-shifting signal is employed for times that are long relative to the time scale for collision, the ions achieve a steady-state distribution of kinetic energies. This distribution is calculated by summing over a representative sample of trajectories that result from random collisions.

In calculating the kinetic energy distribution, we assume that collisions are equally likely to occur at any point in the acceleration period. This assumption is not rigorously correct, since the ion−dipole collision rate constant can decrease by almost 30% across the range of kinetic energies attained in our experiments, and the kinetic energy of any given ion will change over the course of an acceleration period.[23] The error that results, however, is small because the overall kinetic energy

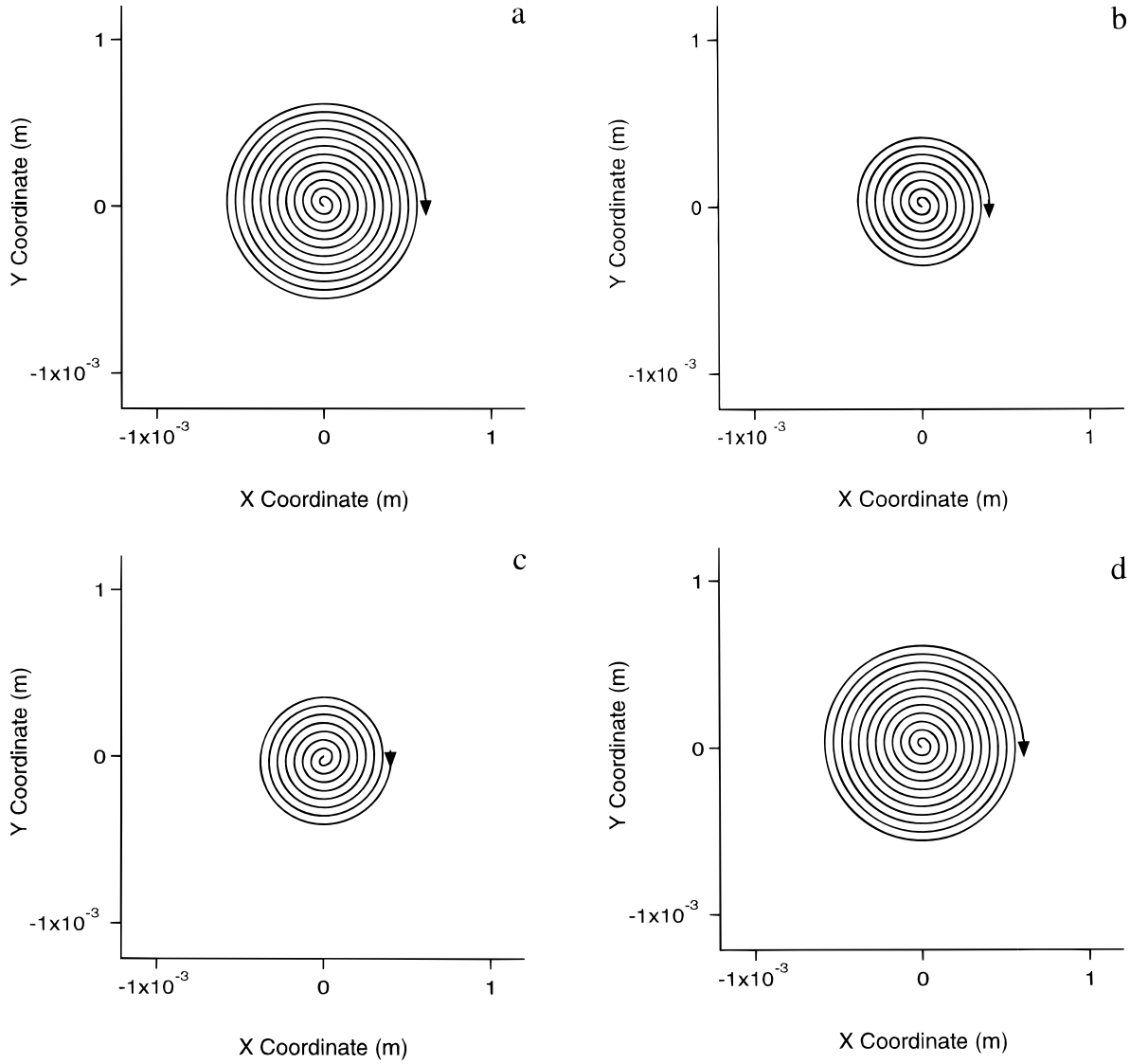

Figure 2. Typical ion trajectory in response to an applied resonant radio frequency, reversed every 20 cycles, in the presence of a bath gas. The motion of the ion is initially similar to that in Figure 1 until the ion collides with a neutral molecule after 12 periods of acceleration (a). For visual clarity, we show the trajectory of an ion that is initially at rest and whose velocity reduces to zero as a result of the collision. In reality, the ion will have a nonzero velocity and an accompanying phase of motion initially and after the collision, and our calculations take this factor into account (see text for details). Although the radius increases with subsequent acceleration (b), the phase of the driving signal reverses after 8 periods of subsequent acceleration so that the ion does not achieve the same maximum velocity as in Figure 1. Once the phase of the rf is reversed, the ion is driven to progressively smaller orbits and reaches the origin after 8 periods of cyclotron motion (c). It then is subsequently driven to larger radii for the remaining 12 periods of the acceleration interval (d), at which point the phase is reversed again. The ion radius will now oscillate between these two limiting radii until another collision occurs, and its overall kinetic energy distribution is considerably lower than it would have been in the absence of any collisions. The magnetic field strength is 0.6 T and the rf field is 16 V m^{-1}. Ion cyclotron motion is clockwise, as indicated by the arrows. The center of each graph, $x = y = 0$, corresponds to the center of ion cyclotron motion, which will move about the cell as a result of the collisions.

distribution remains fairly constant across the period of the driving signal once the majority of ions have undergone collisions (see below).

If the ion and neutral are both atoms, then they behave like hard spheres and the collisions are completely elastic. The average final kinetic energy of the ions is the center-of-mass collision energy, and the velocity will be distributed isotropically among the *x*-, *y*-, and *z*-axes in the center-of-mass frame. The distribution of ϕ_1, the phase of the ion cyclotron motion, will therefore also be isotropic. The *x*- and *y*- components of the velocity determine $v(0)$, and the *z*-axis component is conserved throughout subsequent acceleration until the next collision. By use of these assumptions, ion trajectories may be calculated.

The case of a polyatomic neutral is similar, except that the collisions are no longer completely elastic and some fraction of the collision energy ends up in rotational and vibrational, as well as translational, degrees of freedom. The redistribution of energy determines the final ion velocity and, hence, its radius. Energy partitioning is easily calculated for the limit of statistical inelastic collisions in which energy is partitioned into all modes according to their statistical density of states. For elastic collisions, the scattering angle distribution of the ion after the collision is assumed to be isotropic. Previous work in our laboratory[24] suggests that the redistribution of collision energy into vibrational energy is likely to fall below the statistical limit, especially for short-lived collision complexes. The error incurred from the statistical assumption is likely to be small, however, because nonstatistical energy partitioning will be greatest in systems with few internal degrees of freedom, for which the energy calculated to end up in vibrations is small relative to that calculated for translational and rotational motions. An upper limit for the associated error is obtained from

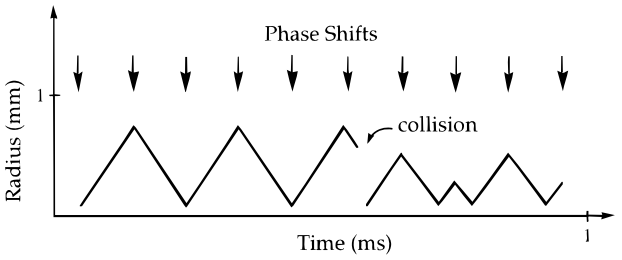

Figure 3. Schematic graph of the effect of a collision on ion radius as a function of time under a periodically phase-reversing rf potential. Downward arrows represent the times at which the phase of the resonant rf is reversed. For visual clarity, the ion trajectory begins with zero velocity and is reduced to zero velocity in the bimolecular collision. In reality, the ion will have a nonzero velocity and associated phase initially and after the collision. Prior to the collision, the ion radius oscillates between zero and a maximum limit defined by the amplitude and width of the acceleration period (see also Figure 1). After a collision in the middle of an acceleration period, the ion radius oscillates between limiting radii that are now less than the maximum radius in the absence of collisions (see also Figure 2).

calculations of ion trajectories using the purely elastic limit, and we find that the choice of energy redistribution model has very little effect (<3%) on the average kinetic energy calculated for representative systems.

Although we do not examine the reactions of polyatomic ions in this work, it is worth considering how their behavior would differ from monotonic ions. Upon collision, accelerated polyatomic ions will become rotationally and vibrationally excited. Unlike neutral collision gases, the excited ions neither diffuse from the cell nor collide with the cell walls, and so they remain internally hot. The distribution of ion internal energies is difficult to calculate because it depends on the rate and average energy of collisions, the efficiency of energy transfer, and the relative rates of reaction (bimolecular and unimolecular) of the ions as a function of energy. We have previously shown that acceleration of polyatomic ions in a phase-shifting rf potential can be used to effect collision-induced dissociation,[13,14] but a rigorous quantitative examination of energy disposal in this technique has not been performed.

Ion Detection. Because an ultimate goal of this acceleration technique is to study the translational dependence of bimolecular reactions, an important concern is whether manipulation of the ion kinetic energies in the manner described above influences the detection of the ions. The potential induced on the detection electrodes by the ions in an FT-ICR (and, therefore, the strength of the ion signal) depends on the final ion position after impulse excitation.[2,6,25] It is possible that changing the ion axial and radial distribution prior to detection influences the position after impulse excitation. We therefore have performed several control experiments to assess the influence of acceleration on ion detection.

(a) Short-term acceleration (2−10 ms) of one ion has no measurable effect on its signal strength relative to nonresonant ions. This implies that differences in signal strength at longer acceleration times are the result of differences in reactivity rather than differential detection.

(b) If two chloride isotopes ($^{35}Cl^-$ and $^{37}Cl^-$) are generated from an unreactive precursor (CCl_4) in the absence of reactive compounds, selective acceleration at low rf potentials does not change the observed isotope ratio even for long acceleration periods. For stronger driving signals ($E_{corr} > 10$ V m^{-1}, $N = 40$), the signal of the resonant ion decreases with time. We are able to conclusively attribute the signal decrease to increased ion loss at higher translational energies and not to differential detection, however, because the isotope ratio remains constant for long delay times (10−1000 ms) between the end of the acceleration signal and the initiation of the detection sequence. At longer delay times, the originally "hot" resonant ions have been cooled by collisions and possess the same thermal translational energy distribution as the nonresonant ions. Since cooling is not observed to influence detection, the reverse must also be true and acceleration from thermal to excited ion motion must not affect detection efficiency.

(c) We have observed that the rate constant of the collision-controlled proton-transfer reaction $F^- + CH_2(CN)_2$ is insensitive to the accelerating signal within experimental uncertainty (±5%) for average kinetic energies below 0.1 eV, and the collision rate of that reaction is calculated[23] to have only a slight (<10%) translational energy dependence over that range of kinetic energy. Because a negligible change in rate is observed for the barrierless reaction of $F^- + CH_2(CN)_2$, we conclude that the more substantial changes observed in slower reactions reflect the energy-dependent dynamics of those systems.

(d) One of the most likely source of detection artifacts would be excitation to different radii of the fast and thermal ions by the impulse excitation event. The ratio of the ion signal to its third harmonic is a measure of the ion radius during detection.[2,3,5,6] We find that under our acceleration conditions, the ratio of the third to first harmonic after impulse excitation is insensitive to the acceleration signal; that is, the average radius after impulse excitation is not measurably influenced by preliminary acceleration/deceleration.

(e) Differential ion loss is a final concern because at higher translational energies we do observe that the resonant ions are ejected from the cell faster than nonresonant ions in some systems (see (b) above). Such ion loss can ultimately lead to considerable error in the measured rate constants. Only data from those systems for which ion loss is slow on the time scale of reaction, therefore, can be reported with confidence. The primary mechanism of ion loss appears to be axial scattering of the ion upon collision with a second body, and the use of suitable trapping potentials (2.8−3.5 V rather than the 1.0−1.5 V typical for our instrument) significantly minimizes such events in our experiments. The use of these somewhat higher trapping potentials is further desirable because Grosshans and Marshall have found that the final ion radius resulting from an applied rf is reproduced more consistently at higher trapping potentials.[4,6]

Although we cannot state conclusively that a preliminary phase-shifting acceleration signal has absolutely no effect on impulse detection in an FT-ICR, the evidence above demonstrates that any such effects are negligible in our experiments. This observation is consistent with the fact that the maximum radial excitation due to acceleration, calculated from eq 1, is a factor of 3−10 smaller than the average radius of the ions after impulse excitation, as estimated from the amplitude of the third harmonic.[4,6] Thus, the final ion packet radius after impulse excitation is relatively unaffected by the perturbations due to the acceleration/deceleration interaction.

Although the use of the acceleration technique in this work did not create any measurable detection artifacts, it would be foolish to generalize that a change in experimental conditions (impulse strength, rf potential, trapping voltage, etc.) would not lead to considerable error in similar experiments. In our opinion, therefore, the use of the kinetic energy controller should in all cases be accompanied by rigorous control experiments.

Experimental Section

Experiments were conducted in an IonSpec OMEGA FTMS Fourier transform ion cyclotron resonance spectrometer (FT-ICR) equipped with a 2 in. cubic stainless steel cell and an

electromagnet operating at 6.0 kG. Background pressure in the vacuum chamber containing the FT-ICR cell was typically 3×10^{-9} Torr. Carbon tetrachloride (Aldrich) and methyl bromide (Matheson) were purged by multiple freeze−pump−thaw cycles prior to use. Reagent gas pressures were measured with a Varian 844 ionization gauge that was calibrated for each gas against an MKS Baratron capacitance manometer. Reagent pressures were typically 3×10^{-7} Torr in CCl_4 and 1×10^{-6} Torr in CH_3Br. Impulse excitation was used to excite the ions prior to detection.

Kinetic Energy Controller. The kinetic energy of the ions was controlled by an rf potential on two electrodes radial to the cyclotron motion of the ions. The signal input was provided by a Hewlett-Packard 3325A frequency synthesizer routed through a device, which we refer to as the ion kinetic energy controller. The function of the ion kinetic energy controller is described below. Acceleration frequencies were kept within 5 Hz of the measured effective cyclotron frequency. The effect of the accelerating signal is to drive ions to progressively larger cyclotron radii and therefore increased kinetic energies.[1,26] Grosshans and Marshall have shown that the resulting radius is overestimated by the infinite electrode approximation,[4,6] and our calculations take this into account. The differential potential of the rf signal used to accelerate the ions was typically in the range 5−30 V m^{-1}.

The acceleration signal, if applied continuously for even fairly short (∼10 ms) time intervals, would simply eject resonant ions from the ICR cell, and it would not be possible to observe changes in reactivity that occur on longer (100 ms to 10 s) time scales. To circumvent this problem, the ion kinetic energy controller manipulates the rf signal so that ions are accelerated for only N cyclotron periods, where N is an integer. At the end of N periods, the phase of the rf signal is reversed by 180°, which drives the ions back to smaller radii and decreased kinetic energies for another N periods of cyclotron motion until the phase of the rf signal is reversed again.[13−15] The ions may be trapped for several seconds, during which time the phase of the rf is reversed at regular intervals. For this work, the interval between phase shifts was kept at $N = 40$. Because the cyclotron frequency of chloride at 6 kG is approximately 2.5×10^5 Hz, each acceleration or deceleration period lasted roughly 1.6×10^{-4} s.

Trajectory Calculations. The trajectory of any ion is determined by its last collision. We therefore calculated total kinetic energy distributions by summing over 600 ion trajectories that originate from a random sample of bimolecular collisions during the phase-reversed irradiation. Because the calculations assume that all the ions in the cell have collided at least once to give the steady state, we delay the start of the bimolecular kinetic data collection until the fraction of ions that have undergone zero collisions is less than 10%.

Each trajectory depends on the point in time within the acceleration/deceleration sequence at which it originated (i.e., when the bimolecular collision occurred), the velocities of the ion and neutral colliders, and the scattering angle of the ion after the collision. For a given ion trajectory, a random number generator determines the moment within the acceleration/deceleration period at which a collision occurs. The timing of the collision determines the velocity of the ion, and the kinetic energy of the neutral is assumed to be the 350 K thermal value (0.045 eV). We assume that the total center-of-mass collision energy is partitioned into the translational, rotational, and vibrational degrees of freedom at or near the statistical average, and a second random number determines how the translational energy is distributed among the *x*-, *y*- and *z*- axes within the center-of-mass frame. The most important function of the second random number is to determine the phase ϕ_1 of the ion. The resulting velocities are converted to the laboratory frame, and eq 1 is then used to calculate the position and kinetic energy of the ion during subsequent acceleration/deceleration periods.

The assumptions regarding energy redistribution and complete collisional rephasing of ion motion could introduce systematic error into the kinetic energy distributions. We have therefore calculated the error that could result from these assumptions by performing trajectory calculations in which (a) the energy redistribution model is varied between the statistical inelastic and completely elastic limits and (b) 10% of the ion trajectories originate from a 350 K distribution of ion kinetic energies at the initiation of the phase-reversing irradiation rather than from a collision during an accelerating period. The model calculations suggest that the resulting error in the calculated average kinetic energy is almost entirely determined by assumption b and should be less than 10%.

Kinetic Measurements. The rate constant of the reaction of $Cl^- + CH_3Br$ as a function of kinetic energy was measured as follows. Chloride ions were generated by electron impact on the neutral carbon tetrachloride, and $^{35}Cl^-$ was subjected to phase-shifting acceleration for several hundred milliseconds in order to achieve a steady-state kinetic energy distribution (see above). The $^{37}Cl^-$ and both isotopes of Br^- were then ejected by standard techniques, isolating the $^{35}Cl^-$. The reaction of $^{35}Cl^-$ with CH_3Br was monitored at a fixed delay time under acceleration potentials of varying strength, and the relative rate constant for reaction was derived for each field strength from the relative amounts of $^{35}Cl^-$ and Br^- in the rf-on vs rf-off experiments. The rate law for disappearance of $^{35}Cl^-$ yields

$$\ln\left[\frac{^{35}Cl^-}{^{35}Cl^- + Br^-}\right] = -kt$$

If the reaction time is held constant, then the ratio of the rf-off rate constant to the rf-on rate constant is given by

$$\frac{k_{\text{rf-on}}}{k_{\text{rf-off}}} = \frac{\ln\left[\frac{^{35}Cl^-}{^{35}Cl^- + Br^-}\right]_{\text{rf-on}}}{\ln\left[\frac{^{35}Cl^-}{^{35}Cl^- + Br^-}\right]_{\text{rf-off}}}$$

Results and Discussion

We have calculated the steady-state kinetic energy distributions of ions in the cell by summing over 600 postcollisional ion trajectories, and the calculated distributions are shown in Figure 4. A histogram of the kinetic energies at the instant that the phase of the driving signal is reversed is shown in Figure 4a, and a histogram of the kinetic energies halfway between two phase shifts is shown in Figure 4b. As seen in the inset of Figure 4, the kinetic energy is higher on average at the beginning or end of an acceleration period than in the middle. This is not surprising, given that half the ions should be at their maximum kinetic energies at the point of the phase shift. Nevertheless, the distribution does not change very much during the time between phase shifts and has achieved, for all practical purposes, a steady state. Because the time interval of an acceleration period (here, 0.16 ms) is very small on the time scale of bimolecular reactions (typically 100−1000 ms), the observed reactivity will reflect the kinetic energy distribution summed across the entire acceleration period. Such a distribution is shown in Figure 5.

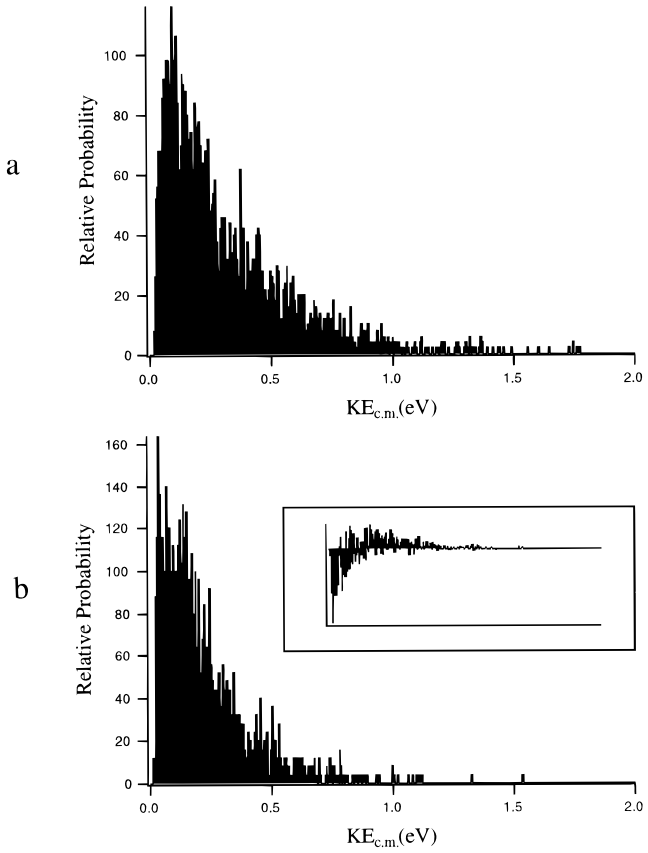

Figure 4. Kinetic energy distributions of 600 random ion trajectories (a) when the phase of the accelerating signal is reversed and (b) at a point halfway between two phase shifts. The inset in (b) is the difference of (b) subtracted from (a). See text for details.

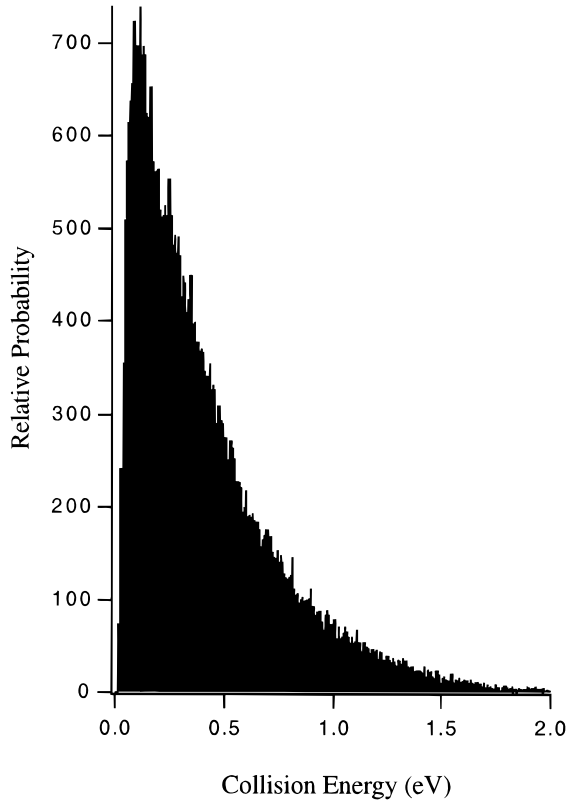

Figure 5. Overall kinetic energy distribution of 600 random ion trajectories summed across the entire period between two phase shifts.

As seen in Figure 5, the complete distribution bears little resemblance to a thermal Maxwell−Boltzmann distribution and thus hinders the direct comparison of the FT-ICR results to those obtained in experiments at an elevated temperature or in another apparatus with a similar average kinetic energy; the effect of the different energy distribution for the two cases must be considered. On the other hand, the kinetic energy distribution is easily calculable, and so the experimental results may be compared to theoretical predictions by averaging the rate constant as a function of kinetic energy over the appropriate distribution function P(KE):

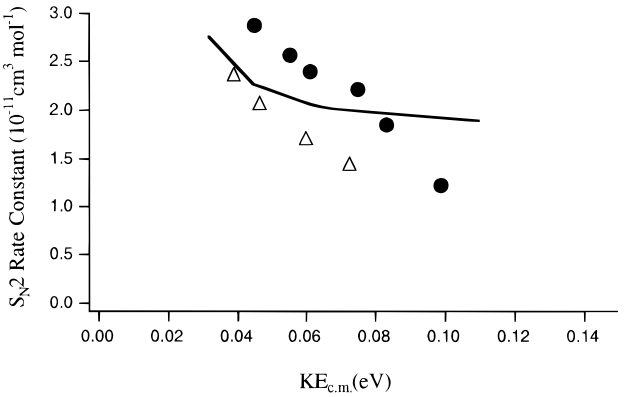

Figure 6. Reaction rate constant of $Cl^- + CH_3Br \rightarrow Br^- + CH_3Cl$ plotted as a function of average center-of-mass collision energy between the reactants. Experimental data are from this work (●) and ref 20 (△). The line (−) is the kinetic energy dependence calculated with RRKM theory (ref 28).

$$k_{obs} = \frac{\int_{KE} P(KE) k(KE)}{\int_{KE} P(KE)} \quad (2)$$

Viggiano and co-workers have previously reported a selected ion flow tube (SIFT) study of the translational energy dependence of the S_N2 reaction in eq 3 in which the rate constant is observed to decrease as the center-of-mass kinetic energy increases over a range 0.03−0.08 eV.[27]

$$Cl^- + CH_3Br \rightarrow Br^- + CH_3Cl \quad (3)$$

To test the FT-ICR acceleration technique, we have performed similar experiments on the reaction in eq 3. The results of this work are plotted as a function of average center-of-mass kinetic energy in Figure 6. The 350 K thermal rate constant of 2.8×10^{-11} cm^3 mol^{-1} obtained in this study agrees quite well with the 300 K value of 2.4×10^{-11} cm^3 mol^{-1} (2.2×10^{-11} cm^3 mol^{-1} at 350 K, by extrapolation) reported previously by Viggiano, given the 25−30% error associated with absolute rate measurements in the two instruments.

Of more interest is the quantitative kinetic energy dependence of the rate constant. As observed by Viggiano, the rate of the reaction decreases essentially linearly with increasing kinetic energy over this range of kinetic energy. Because the rate of the reaction varies linearly with kinetic energy for eq 3, the results of our study may be compared directly to those obtained in the earlier work (see Appendix below).

The two independent measurements of the kinetic energy dependence are in excellent agreement, since the linear least-squares fits of rate constant vs collision energy have nearly identical slopes of -2.72×10^{-10} cm^3 mol^{-1} eV^{-1} (SIFT) and -2.86×10^{-10} cm^3 mol^{-1} eV^{-1} (ICR), a difference of 5% that is within the relative uncertainty in each of the experiments. This suggests that the energy dependence of eq 3 is independent of the pressure difference between the SIFT (∼0.5 Torr) and ICR (∼10^{-6} Torr). As shown in Figure 6, the measured kinetic

energy dependence is much greater than that predicted by RRKM theory, as calculated by Wang and Hase,[28,29] and implies "nonstatistical" dynamics in the reaction of eq 3, especially at higher (>0.05 eV) collision energies. This result is consistent with other studies of energy disposal in eq 3,[30,31] and the implications of such behavior have been discussed thoroughly in prior work in our laboratory and by others.[27,28,30−38]

A translationally excited ion population can also be achieved using another methodology, most notably the sustained off-resonance irradiation (SORI) technique developed by Jacobson, which has been used successfully in low-energy collision-induced dissociation studies.[39] To our knowledge, SORI has not been applied to the study of bimolecular reaction kinetics, but it is a continuous process and should generate a steady-state kinetic energy distribution. The equations of motion for ions undergoing SORI are known, and the total kinetic energy distribution should be calculable. As in our method, the kinetic energy of ions accelerated using SORI varies between upper and lower limits. As Jacobson points out, an analysis of the ion kinetic energy becomes complicated as the time interval between minimum and maximum kinetic energies approaches the time scale of bimolecular collision. In our technique, the duration of the acceleration interval is determined by *N*, the number of cyclotron periods between phase shifts, and the cyclotron frequency of the resonant ion. In SORI, it depends upon the difference in the frequencies of the ion and the irradiating signal.

To be useful, an ion acceleration technique must meet the following criteria. (1) The steady-state distribution of kinetic energies should be narrow enough to be useful and theoretically or experimentally well-characterized. We are unable to characterize the kinetic energy distribution experimentally, and the possibility of systematic error exists. The theoretical characterization, however, is based upon known equations of motion, and test calculations demonstrate that the average kinetic energy is only slightly sensitive (±10%) to the treatment of energy redistribution and the assumptions of complete collisional rephasing of ion motion. Although the distribution is not Maxwell−Boltzmann, it is calculable, and studies using the phase-shifting acceleration technique can be compared to theory or other experiments by considering the appropriate distribution of energies. (2) The range of accessible kinetic energies should be large enough to be useful, and so far we have obtained reproducible results up to approximately 0.3 eV average ion kinetic energy. (3) The technique should be accurate and reproducible. Although optimization of instrumental parameters (trapping voltages, ion signal strength, impulse detection waveform) is nontrivial in our instrument, rigorous control experiments verify that artifacts are not introduced into the rate measurements using the phase-reversing technique. Furthermore, our study of the S_N2 reaction of $Cl^- + CH_3Br$ accurately reproduces results obtained in a previous study of that reaction.

Conclusions

The use of a phase-shifting resonant rf signal to achieve an accelerated steady-state ion kinetic energy distribution in an ICR has been described. This technique is viable at the low (10^{-7}−10^{-5} Torr) pressures in an ICR and thus facilitates the study of the translational energy dependence of bimolecular reactions in such conditions. The distribution of ion kinetic energies in the steady state, although not known exactly, is calculable to reasonably high precision. Rigorous control experiments have been used to show that, for the experimental and detection conditions employed in this work, the acceleration technique does not affect the detection of the resonant ions. Results obtained for the reaction of $Cl^- + CH_3Br$ are in excellent agreement with those obtained in a previous SIFT study of that reaction. These results demonstrate that the phase-shifting acceleration technique represents a viable means of studying the translational energy dependence of bimolecular ion−molecule reactions at low pressure.

Acknowledgment. We are grateful to the National Science Foundation for support of this research. S.L.C. acknowledges fellowship support from the National Science Foundation, the ACS Division of Organic Chemistry (DuPont Merck Pharmaceutical Fellowship), and Stanford University (John Stauffer Memorial Fellowship). We thank M. Chabinyc and Professor E. Williams for helpful discussions.

Appendix

The average collision energy of the reactants is obtained by summing over the appropriate energy distribution

$$\langle \mathrm{KE} \rangle = \frac{\int_{\mathrm{KE}} P(\mathrm{KE}) \times \mathrm{KE}}{\int_{\mathrm{KE}} P(\mathrm{KE})}$$

and the observed rate constant is

$$k_{\mathrm{obs}} = \frac{\int_{\mathrm{KE}} P(\mathrm{KE}) k(\mathrm{KE})}{\int_{\mathrm{KE}} P(\mathrm{KE})}$$

but since $k(\mathrm{KE}) = C \times \mathrm{KE}$,

$$k_{\mathrm{obs}} = \frac{\int_{\mathrm{KE}} P(\mathrm{KE}) \times C \times \mathrm{KE}}{\int_{\mathrm{KE}} P(\mathrm{KE})} = \frac{C \int_{\mathrm{KE}} P(\mathrm{KE}) \times \mathrm{KE}}{\int_{\mathrm{KE}} P(\mathrm{KE})}$$

Plots of average rate constant vs average center-of-mass kinetic energy for eq 3, therefore, will be independent of the kinetic energy distribution in the range of energies for which rate varies linearly with kinetic energy.

References and Notes

(1) Beauchamp, J. L. *Annu. Rev. Phys. Chem.* **1971**, *22*, 527.
(2) Rempel, D. L.; Huang, S. K.; Gross, M. L. *Int. J. Mass. Spectrom. Ion Processes* **1986**, *70*, 163−184.
(3) van der Hart, W. J.; van de Guchte, W. J. *Int. J. Mass. Spectrom. Ion Processes* **1988**, *82*, 17−31.
(4) Grosshans, P. B.; Marshall, A. G. *Int. J. Mass. Spectrom. Ion Processes* **1990**, *100*, 347−379.
(5) Grosshans, P. B.; Shields, P. J.; Marshall, A. G. *J. Am. Chem. Soc.* **1990**, *112*, 1275.
(6) Grosshans, P. B.; Marshall, A. G. *Int. J. Mass. Spectrom. Ion Processes* **1992**, *115*, 1−19.
(7) Burnier, R. C.; Cody, R. B.; Freiser, B. S. *J. Am. Chem. Soc.* **1982**, *104*, 7436.
(8) Cody, R. B.; Burnier, R. C.; Freiser, B. S. *Anal. Chem.* **1982**, *54*, 96.
(9) Kofel, P.; McMahon, T. B. *Int. J. Mass. Spectrom. Ion Processes* **1990**, *98*, 1.
(10) Hop, C. E. C. A.; McMahon, T. B.; Willett, G. D. *Int. J. Mass. Spectrom. Ion Processes* **1990**, *101*, 191.
(11) Hop, C. E. C. A.; McMahon, T. B. *J. Phys. Chem.* **1991**, *95*, 10582−10586.
(12) Wilkinson, F. E.; Hop, C. E. C. A.; McMahon, T. B. *Chem. Phys. Lett.* **1992**, *192*, 517−521.
(13) Boering, K. A.; Rolfe, J.; Brauman, J. I. *Rapid Commun. Mass Spectrom.* **1992**, *6*, 303−305.
(14) Boering, K. A.; Rolfe, J.; Brauman, J. I. *Int. J. Mass. Spectrom. Ion Processes* **1992**, *117*, 357−386.
(15) Marshall, A. G.; Lin Wang, T.-C.; Lebatuan Ricca, T. *Chem. Phys. Lett.* **1984**, *105*, 233−236.
(16) Kleingeld, J. C.; Nibbering, N. M. M. *Tetrahedron* **1983**, *39*, 4193.

(17) Noest, A. J.; Kort, C. W. F. *J. Comput. Chem.* **1983**, *7*, 81.
(18) Vulpius, T.; Houriet, R. *Int. J. Mass. Spectrom. Ion Processes* **1989**, *88*, 283−290.
(19) Hanson, C. D.; Kerley, E. L.; Russell, D. H. *Anal. Chem.* **1989**, *61*, 83.
(20) Pfandler, P.; Bodenhausen, G.; Rapin, J.; Houriet, R.; Gaumann, T. *Chem. Phys. Lett.* **1987**, *138*, 138.
(21) Pfandler, P.; Bodenhausen, G.; Rapin, J.; Walser, M. *J. Am. Chem. Soc.* **1988**, *110*, 5625.
(22) Hearn, B. A.; Watson, C. H.; Baykut, G.; Eyler, J. R. *Int. J. Mass. Spectrom. Ion Processes* **1990**, *95*, 299−316.
(23) Su, T. *J. Chem. Phys.* **1994**, *100*, 4703.
(24) Boering, K. A.; Brauman, J. I. *J. Chem. Phys.* **1992**, *97*, 5439.
(25) Dunbar, R. C. *Int. J. Mass. Spectrom. Ion Processes* **1984**, *56*, 1−9.
(26) Freiser, B. S.; Farrar, J. M.; Saunders, W. H. J. *Techniques for the Study of Ion-Molecule Reactions;* Wiley-Interscience: New York, 1988.
(27) Viggiano, A. A.; Morris, R. A.; Paschkewitz, J. S.; Paulson, J. F. *J. Am. Chem. Soc.* **1992**, *114*, 10477.
(28) Wang, H.; Hase, W. L. *J. Am. Chem. Soc*. **1995**, *117*, 9347−9356.
(29) The data plotted in Figure 6 differ from a similar plot in Figure 2 of ref 28. The experimental data in the latter graph were plotted incorrectly; correct data are shown here. As seen in Figure 6, however, the conclusions of ref 28 regarding nonstatistical behavior in eq 3 are still valid (Wang, H.; Hase, W. Personal communication).
(30) Graul, S. T.; Bowers, M. T. *J. Am. Chem. Soc.* **1991**, *113*, 9696−9697.
(31) Graul, S.; Bowers, M. T. *J. Am. Chem. Soc.* **1994**, *116*, 3875.
(32) Vande Linde, S. R.; Hase, W. L. *J. Am. Chem. Soc.* **1989**, *111*, 2349−2351.
(33) Vande Linde, S. R.; Hase, W. L. *J. Phys. Chem.* **1990**, *94*, 6148−6150.
(34) Vande Linde, S. R.; Hase, W. L. *J. Chem. Phys.* **1990**, *93*, 7962.
(35) Viggiano, A. A.; Morris, R. A.; Su, T.; Wladkowski, B. D.; Craig, S. L.; Zhong, M.; Brauman, J. I. *J. Am. Chem. Soc.* **1994**, *116*, 2213−2214.
(36) Hase, W. L. *Science* **1994**, *266*, 998−1002.
(37) Wang, H.; Peslherbe, G. H.; Hase, W. L. *J. Am. Chem. Soc.* **1994**, *116*, 9644.
(38) Viggiano, A. A.; Morris, R. A. *J. Phys. Chem.* **1996**, *100*, 19227−19240.
(39) Gauthier, J. W.; Trautman, T. R.; Jacobson, D. B. *Anal. Chim. Acta* **1991**, *246*, 211.